Quasi-Conformal Transformation Optics (QCTO) enabled modified Luneburg lens design using broadband anti-reflective layer

Soumitra Biswas[1] and Mark Mirotznik[1]
1. Electrical and Computer Engineering Department, University of Delaware, Newark, DE, USA

Introduction

This paper presents a new design methodology of quasi-conformal transformation optics (QCTO) based modified Luneburg lens antennas using a broadband anti-reflective (AR) layer. The design used QCTO technique to modify the spherical Luneburg lens geometry into a flat surface. Electromagnetic structure designed using QCTO technique suffer from reflection problems and to mitigate the impedance mismatches present in QCTO technique, we designed a novel broadband anti-reflective layer along with the QCTO-enabled flat Luneburg lens antenna. The anti-reflective layer based QCTO design methodology was validated by designing and fabricating an example lens antenna to operate in the Ka-band (26GHz – 40GHz). The anti-reflective layer enabled QCTO Luneburg lens antenna was able to achieve a wide beam scanning angle (-55˚ to +55˚) with a good impedance matching across the entire planar excitation surface resulting in an aperture efficiency improvement from less than 20% to 70%.

Introduction

Modern satellite and radar communication systems require wide angle and agile beam scanning elements that combine high gain, high angular resolution, multiband operability and, if possible, low fabrication costs [1]. To achieve these goals, graded-index (GRIN) dielectric lens antennas are an attractive choice for use as low-cost, wide angle and wideband beamforming and beam scanning elements [1-3].

Amongst the variety of GRIN lenses that have been explored so far, the Luneburg lens geometry is the most widely used. The Luneburg lens is a spherical shaped graded dielectric structure in which every point on the lens's surface acts as a focal point for a plane wave incident from the opposite surface and beam scanning is achieved by simply changing between an array of antenna feeds placed along the lens's spherical surface. When implementing this design, however, there is practical challenge. The lens's spherical shape complicates the integration of feed networks and other associated electronics. To address these geometry mismatch issue, most investigators including we, used quasi-conformal transformation optics (QCTO) to modify the surface of Luneburg lens into planar one and optimize the permittivity distribution to ensure an unchanged beam scanning functionalities [1-7]. However, due to the absence of magnetic responses assumed in QCTO technique, these designs are limited by the impedance mismatch problem and resulted in poor performance.

To address these reflection problems associated with QCTO technique, we designed and implemented a broadband anti-reflective layer along with QCTO enabled modified Luneburg lens antenna. The anti-reflective layer has an inhomogeneous permittivity distribution and minimizes the impedance mismatches at every point of the QCTO lens's excitation surface. An example lens with anti-reflective layer was designed and fabricated to operate in the Ka-band. The lens showed a good beam steering performance from (-55˚ to +55˚) with a good impedance matching across the entire planar surface of the QCTO Luneburg lens.

QCTO modified Luneburg lens design

To modify the portion of the Luneburg lens's spherical geometry into a flat surface and calculate the new material parameters, a two-dimensional coordinate transformation of the original 2D Luneburg lens was carried out by solving Laplace's equations in the transformed space with a set of Dirichlet and Neumann boundary conditions [1-2]. The new material parameters of the modified Luneburg lens antenna were calculated following the quasi-conformal transformation optics (QCTO) protocol for inverse coordinate transformation [1-2]:

$$\varepsilon' = \frac{\varepsilon_r}{|\boldsymbol{\Lambda}^{-1}|}; \quad \mu' = 1$$

Figure 1(a) shows the permittivity distribution of the original two-dimensional Luneburg lens, and figure 1(b) presents the modified permittivity distribution of the QCTO-enabled two-dimensional Luneburg lens. The quasi-conformal mapping and calculation of the material parameters were implemented using

COMSOL™ solver. The three-dimensional implementation of the QCTO-enabled modified Luneburg lens was achieved by revolving the two-dimensional permittivity distribution (figure 1(b)) along its center axis (z-axis) following the method described in [6]. Figure 1(c) demonstrates the three-dimensional permittivity distribution of QCTO modified Luneburg lens antenna.

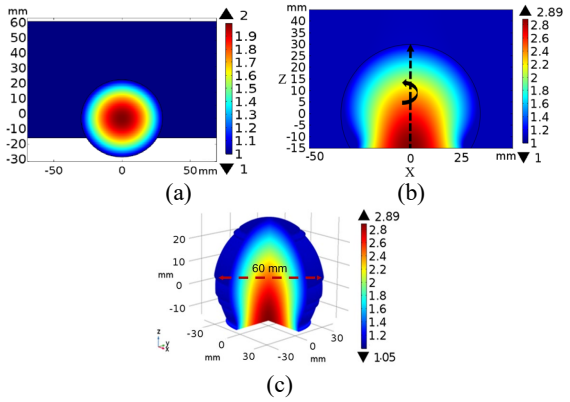

Figure 1: Permittivity profile for (a) cross sectional view of 2D original Luneburg lens, (b) cross sectional view of 2D modified Luneburg lens, (c) 3D representation of modified Luneburg lens permittivity distribution

Anti-Reflective layer design:

The three-dimensional design of QCTO modified Luneburg lens assumes the material parameters as all-dielectric and non-magnetic in nature, and such an approximation results in reflections at the lens's excitation boundary due to the presence of impedance mismatches. To Ensure a uniform impedance matching across the lens's entire planar excitation surface (figure 1(c)), a broadband anti-reflective (AR) layer was designed. The AR layer has a continuously tapered permittivity profile which minimizes the mismatches at every single point and the permittivity profile was calculated using the following formula [1,8]:

$$\sqrt{\varepsilon_{AR}(x,z)} = \sqrt{\varepsilon_i \varepsilon_s(x,z)}\,\exp\left[\Gamma_m A^2\,\Phi\left(2\frac{z}{L}-1, A\right)\right]; \quad \text{for } 0 \le z \le L$$

Here $\varepsilon_s(x, z)$ is the permittivity distribution of QCTO Luneburg lens's planar surface (figure 1b) and ε_i has the permittivity distribution of air. L represents the thickness of the anti-reflective layer and for this specific design, it was considered as $\lambda/2$ at the lowest frequency of ka-band (26 GHz). The permittivity distribution of the AR layer was calculated by using COMSOL-MATLAB interface as shown in figure 2(a). Figure 2(b-d) presents the variation of permittivity value across the AR layer thickness in 2D and 3D.

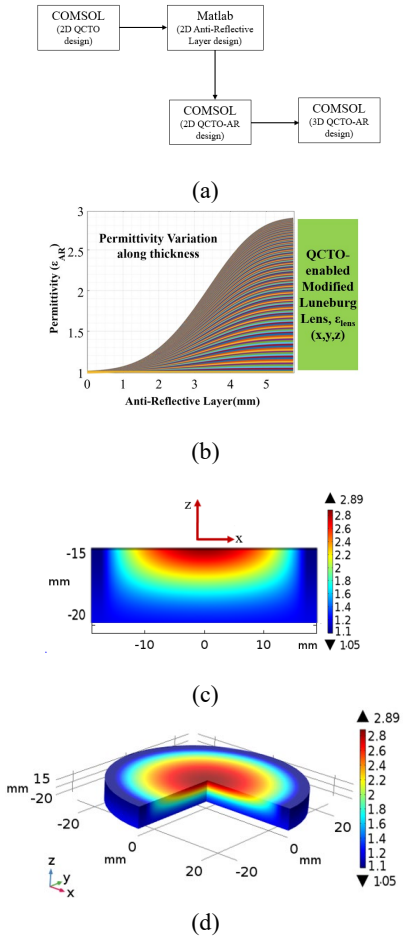

Figure 2: Anti-reflective layer design: (a) Anti-reflective design methodology using COMSOL™-MATLAB interface; (b) graphical representation of tapered permittivity distribution along the AR layer thickness; (c) 2D surface profile of AR layer's permittivity distribution; (d) axisymetrically rotated 3D permittivity distribution of AR layer

Figure 3 represents the permittivity distribution of the three-dimensional QCTO Luneburg lens antenna, with and without the presence of an anti-reflective layer at the bottom planar excitation surface.

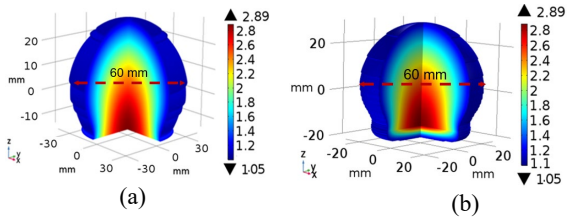

Figure 3: 3D QCTO modified Luneburg lens: (a) conventional QCTO lens without an anti-reflective layer, (b) QCTO lens with the presence of an AR layer

3D Full-wave simulations:

To show the beam steering performances and gain patterns of the modified lens antenna with the presence of an AR layer, 3D full-wave electromagnetic simulations were carried out using COMSOL™ numerical solver. To demonstrate the beam steering performances of the design, the lens's planar surface (figure 3b) was excited with a waveguide port using the simulation setup shown in figure 4. The lens was excited at five locations (figure 5a) with an open-ended waveguide, and at each location 3D radiation patterns were calculated using COMSOL solver. Figure 5 (b-f) presents the simulated radiation patterns of the anti-reflective layer enabled modified Luneburg lens antenna at 30 GHz. It is clear that the lens shows a beam steering performance from -55 ˚ to +55 ˚.

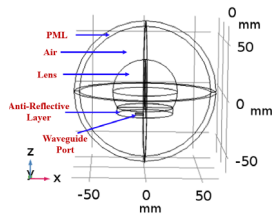

Figure 4: COMSOL simulation setup

Figure 6 compares the simulated gain patterns of the lens antennas as a function of beam steering angle with and without the presence of an AR layer for three feed locations (pos -2, pos -1, pos 0) at 30 GHz. It is evident that the AR layer enabled QCTO Luneburg lens (figure 3b) shows equivalent beam steering performance (from -55˚ to +55˚) like that of the lens without an AR layer (figure 3a). However, the presence of the AR layer improved the gain value significantly and the AR layer enabled lens had a flat gain patterns at all excitation locations compared to the lens without an AR layer which resulted in degraded gain patterns due to the reflections.

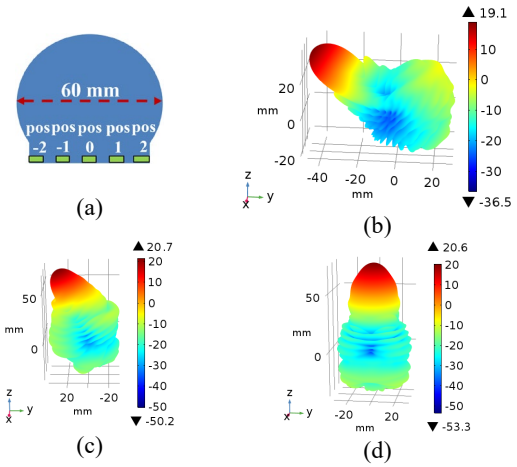

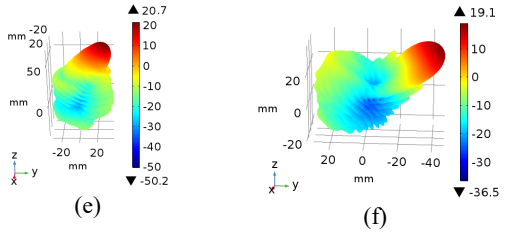

Figure 5: Simulated 3D radiation patterns (dBi) of anti-reflective layer enabled QCTO modified Luneburg lens antenna at 30 GHz for five feed locations

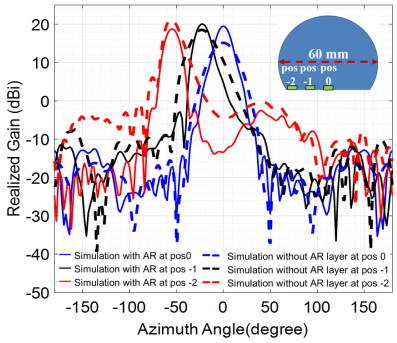

Figure 6: Simulated gain patterns of the modified Luneburg lens antenna (at 30 GHz) with and without the presence of an anti-reflective layer for feed locations at pos -2, pos -1, and pos 0

The lens antenna with anti-reflective layer was fabricated using additive manufacturing technique and experimentally characterized. Space filling curve based additive fabrication method was applied to realize continuously graded dielectric permittivity of the lens antenna [1,7]. Figure 7a compares the simulated and measured gain patterns of the lens antenna with and without the presence of AR layer at three feed locations (pos -2, pos -1, pos 0) at 30 GHz and figure 7b presents the fabricated lens antenna. As expected, the measured gain value of the modified lens antenna with an AR layer increased significantly compared to the lens without an AR layer and had an almost flat gain pattern at all the excitation positions confirming the uniform impedance matching across the entire planar surface of the modified lens structure.

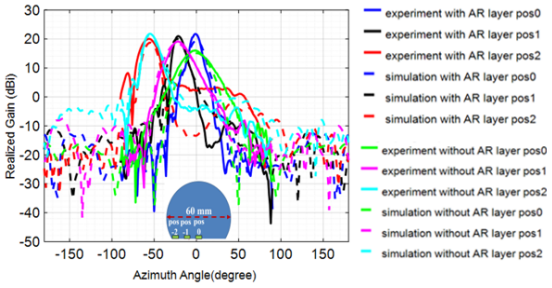

(a)

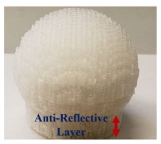

(b)

Figure 7: (a) Measured and simulated gain patterns of the modified Luneburg lens antenna with and without the presence of an anti-reflective layer at 30 GHz for three feed locations (pos -2, pos -1, pos 0); (b) Fabricated lens antenna

Conclusions

In this paper, we presented a new design methodology of quasi-conformal transformation optics (QCTO) based modified Luneburg lens antenna. The method used a novel broadband anti-reflective layer along with QCTO enabled flat Luneburg lens antenna to mitigate the impedance mismatches resulted from QCTO approximation. The design method was validated by designing and fabricating an anti-reflective layer enabled modified Luneburg lens antenna designed to operate in the Ka-band. The antenna performances were measured experimentally and presented to compare well to the simulated results using COMSOL solver. The lens antenna showed a good beam steering from performance (i.e. -55 ˚ to +55 ˚) over the entire Ka-band. We believe, this new anti-reflective layer-based design methodology provides a better means of designing conventional QCTO-enabled devices which suffer from degraded performances due to the high impedance mismatches.

References

1. Soumitra Biswas. Design and additive manufacturing of broadband beamforming lensed antennas and load bearing conformal antennas. *PhD Thesis, University of Delaware*, 2019

2. Biswas S. et al. Realization of modified Luneburg lens antenna using quasi- conformal transformation optics and additive manufacturing. *Microw. Opt. Technol. Lett*. **61,** 1022-1029 (2019)

3. Soumitra Biswas and Mark S. Mirotznik. Customized shaped Luneburg lens design by additive fabrication. 18th International Symposium on Antenna Technology & Applied Electromagnetics (ANTEM), 1-2 (2018)

4. Soumitra Biswas and Mark Mirotznik. 3D modeling of transformation optics based flattened Luneburg lens using Comsol multiphysics modeling software. *Comsol Conference*, 2018

5. Kundtz, N. & Smith, D. R. Extreme-angle broadband metamaterial lens. *Nat. Mater.* **9,** 129–132 (2010)

6. Ma, H. F., & Cui, T. J. Three-dimensional broadband and broad-angle transformation-optics lens. *Nat. Commun.* **1,** 124 (2010).

7. Soumitra Biswas, Zachary Larimore, Mark Mirotznik. Additive Manufactured Luneburg lens based conformal beamformer. 2018 IEEE APS/URSI Conference, Boston, MA, USA

8. Grann, E.B., Moharam, M.G. & Pommet, D.A. Optimal design for antireflective tapered two-dimensional subwavelength grating structures. JOSA A 12, 333-339 (1995).